Supplementary material

Scanning Electron Microscopy (SEM)

Electron microscopy was performed in a Zeiss Merlin FE-SEM, equipped with a Gemini II column (Carl Zeiss, 2008). Imaging of the samples was realized using the In-Lens detector and low acceleration voltages of 600 V to 2 kV, probe current 60 pA. Samples were not modified or treated for the SEM analysis.

Figure 1 presents SEM images for the 35c catalyst with and without thermal annealing (images a and b). Without thermal annealing, the surface remains smooth, whereas with the thermal annealed catalyst, the surface is roughened. These images suggest that thermal annealing modifies the deposited overcoat from a conformal layer to a roughened and nanoporous structure.
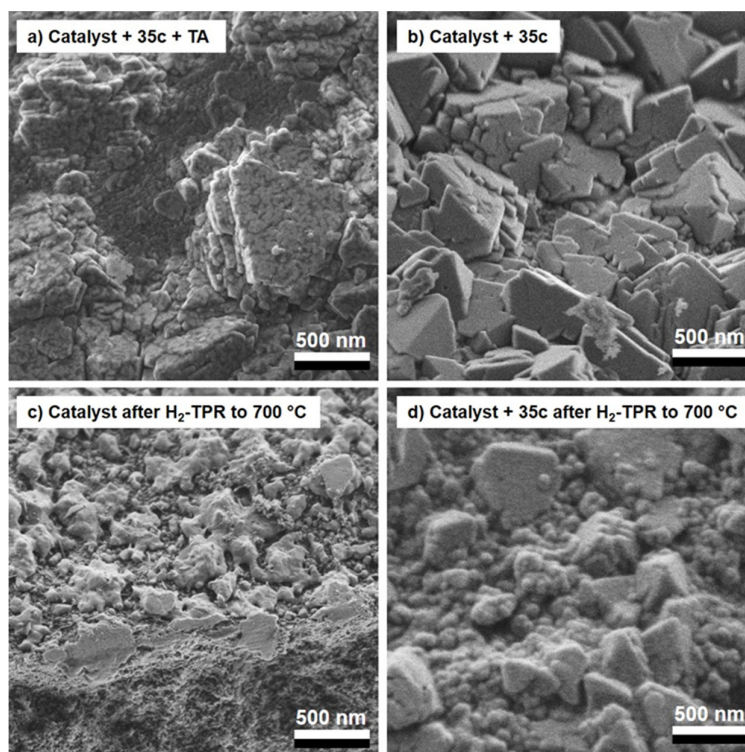

Figure 1. SEM images for catalyst samples a) 35 cycles alumina ALD overcoated catalyst + thermal annealing (TA), b) 35 cycles alumina ALD overcoated catalyst, no TA, c) H_2-TPR to 700 °C for non-top-coated catalyst, d) H_2-TPR to 700 °C for 35 cycles alumina ALD overcoated.

Figure 1, images c and d, show catalysts subjected to temperature-programmed reduction until 700 °C. SEM images taken of catalyst samples after exposure to TPR reveal the effect of the added overcoating. Without overcoating the surface sinters quite severely (image c), whereas with overcoating the characteristic surface features before TPR remain.

Transmission Electron Microscopy (TEM)

For morphology and microstructure characterization, transmission Electron Microscope (TEM) analysis was carried out with TALOS F200X FEG (S) TEM (Thermo Fisher Scientific). Figure 2 present TEM images from non-overcoated catalyst having clear crystalline γ-Al_2O_3 lattice structures and darker cobalt particles. Figure 3 presents similar image set from 35 cycle overcoated catalyst, where ALD overcoating cannot be separately detected from catalyst support.
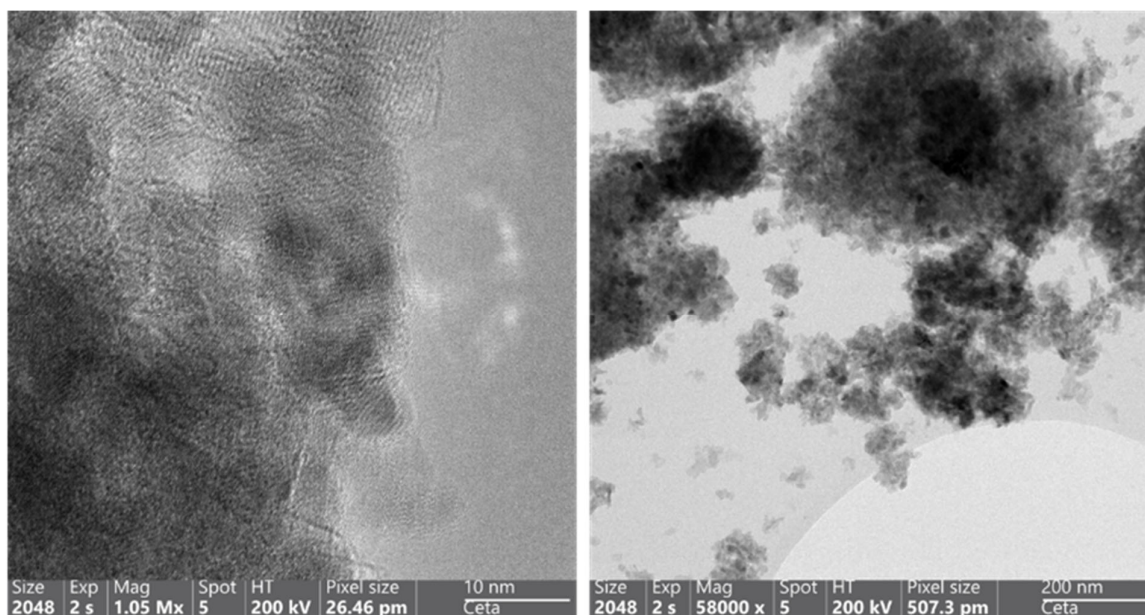

Figure 2. TEM images of Co-Pt-Si/γ-Al_2O_3 without ALD overcoating. Dark areas in both images represent cobalt species.
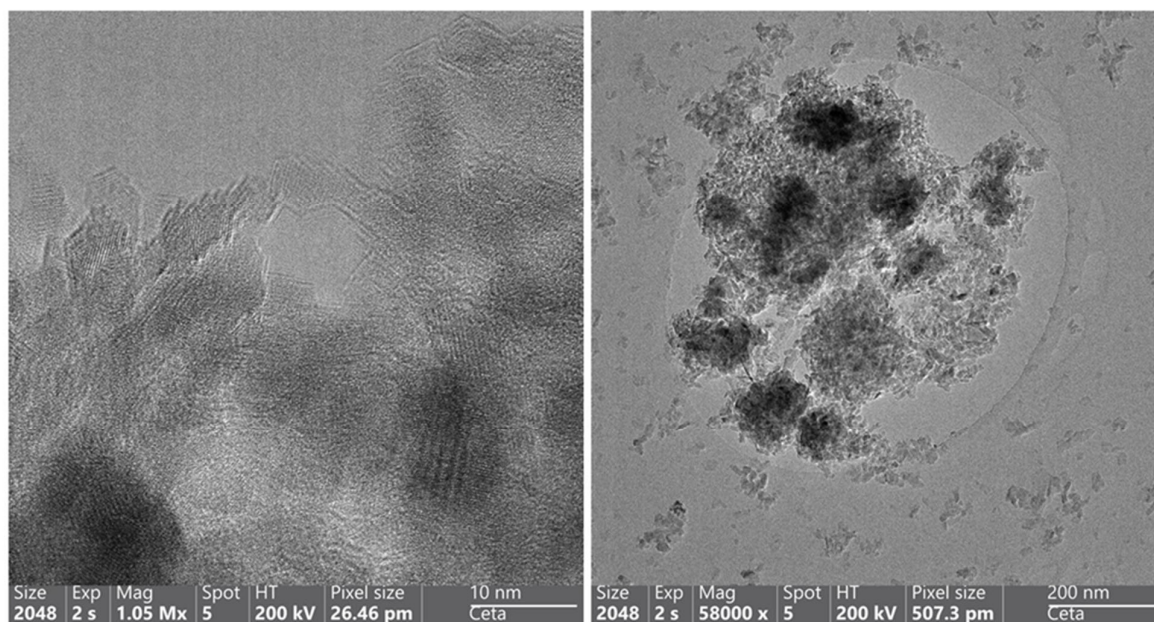
Figure 3. TEM images of Co-Pt-Si/γ-Al$_2$O$_3$ with 35 cycle ALD overcoating. Dark areas in both images represent cobalt species.

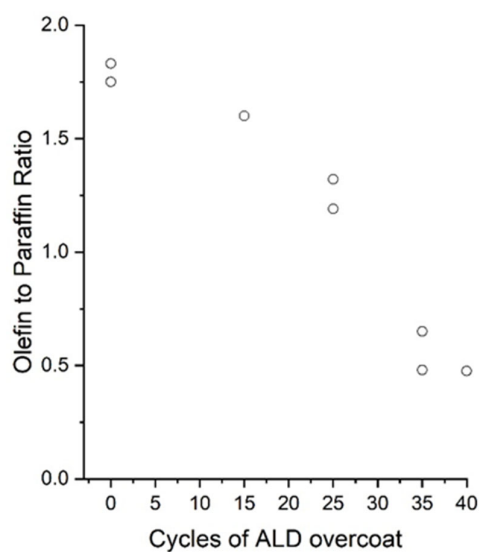**ALD overcoat effect on Olefin-Paraffin ratio**

Figure 4. ALD overcoating and thermal annealing effect on olefin-paraffin ratio for C$_4$-C$_6$ hydrocarbons. Ratio taken after initial activity phase (40 h time-on-stream for all catalysts).

Figure 4 shows a notable decrease in total olefin amount as a function of overcoating thickness. Although the O/P ratio decreased significantly, the ratio of α-olefin to total olefin amount was relatively constant (Table 1). Table 1 gives the ratio between olefin compounds and the dodecanol to C_{12} paraffin ratio. From these results it was apparent that the catalyst + 35c + TA favours olefin isomers, without affecting alcohol products. Although a significant O/P ratio decrease is observed (Figure 4), the rather high cobalt catalyst O/P ratio could result from low conversion level during the experiments and the carrying out of sample analysis after the initial activity phase.

Table 1. Ratios of α-olefin to corresponding paraffin and C_{12} alcohol to corresponding paraffin. Results calculated from C_{12} hydrocarbon and oil samples collected from cold trap. Anderson–Schulz–Flory α-value calculated from C_{30}-C_{60} wax fraction analysis results.

Catalyst	Ratio of C_{12} α-olefin to total C_{12} olefins (wt-%)	Ratio of C_{12}OH to n-C_{12} (wt-%)	ASF α-value
Catalyst	87.2	1.71	0.903
Catalyst + 15c + TA	88.3	1.43	0.886
Catalyst + 25c + TA	83.6	1.57	0.892
Catalyst + 35c + TA	80.6	1.36	0.896
Catalyst + 35c	92.0	0.85	0.894
Catalyst + 40c + TA	85.5	1.54	0.903